Title

Range of Pulmonary Autograft Responses to Systemic Pressure Immediately After Ross Procedure.

Journal

The Journal of Heart Valve Disease, 28(1)

ISSN

0966-8519

Authors

Wisneski, Andrew D
Wang, Zhongjie
Xuan, Yue
et al.

Publication Date

2019

Peer reviewed

HHS Public Access

Author manuscript

J Heart Valve Dis. Author manuscript; available in PMC 2021 November 15.

Published in final edited form as:

J Heart Valve Dis. 2019 ; 28(1): 22–31.

Range of Pulmonary Autograft Responses to Systemic Pressure Immediately After Ross Procedure

Andrew D. Wisneski, M.D.[1], **Zhongjie Wang, Ph.D.**[1], **Yue Xuan, Ph.D.**[1], **Julius M. Guccione, Ph.D.**[1], **Liang Ge, Ph.D.**[1], **Elaine E. Tseng, M.D.**[1]

[1]Department of Surgery, University of California San Francisco (UCSF) and San Francisco Veterans Affairs Medical Center (SFVAMC), San Francisco, CA, USA

Abstract

Background: Pulmonary autograft dilatation after Ross operation often necessitates reoperation. To understand autograft remodeling, a biomechanical understanding of human autografts after exposure to systemic pressure is required. We previously developed an *ex vivo* human pulmonary autograft finite element (FE) model to predict wall stress after exposure to systemic pressure. However, autograft material properties vary significantly among individuals. Our study aim was to quantify range of wall stress changes in a human autograft after Ross operation prior to remodeling based upon normal variation in human autograft mechanical properties.

Methods: A normal human autograft FE model was loaded to pulmonary and systemic arterial pressures. Stress-strain data of normal human autografts (n=24) were incorporated into an Ogden hyper-elastic model to describe autograft mechanical behavior. Autograft wall stresses at pulmonary vs. systemic pressures were examined. Autograft volume-based stress analysis was performed, based on percentage of autograft element volume exceeding 1 standard deviation (SD) above group mean stress at systemic systole.

Results: Mean first principal wall stresses (FPS) at systole of systemic versus pulmonary pressures were 129.29±17.47kPa versus 24.42±3.85kPa ($p<0.001$) at the annulus, 187.53±20.06kPa versus 35.98±2.15kPa at sinuses ($p<0.001$), and 268.68±23.40kPa versus 50.15±5.90kPa ($p<0.001$) at sinotubuluar junction (STJ). The percentage of autograft element volume that exceeded one SD above the group mean was 14.3±5.6% for FPS and 12.6±10.1% for second principal stresses.

Conclusion: We quantified normal human autograft biomechanical responses to systemic pressure based on patient-specific material properties. Regions of peak stresses were observed in autograft sinuses and STJ regions, which corresponded clinically to locations of autograft dilation. Our results provide valuable information on predicting variations in patient-specific *ex vivo* FE models when population-based material properties are used in settings where patient-specific properties are unknown.

Keywords

pulmonary autograft; autograft dilatation; Ross procedure; finite element analysis

Corresponding Author: Andrew Wisneski, M.D., Department of Surgery, UCSF Medical Center, 500 Parnassus Ave., Suite 405W, Box 0118, San Francisco, CA 94143-0118, USA., Phone: 415-221-4810 x23452, Fax: 415-750-2181., Andrew.wisneski@ucsf.edu.

Introduction

The Ross procedure utilizes patient's native pulmonary valve to replace diseased aortic valve(1). It serves as an alternative to mechanical valve replacement and offers numerous benefits including excellent hemodynamics, freedom from anticoagulation, and ability of valve to grow with patient when performed in children or young adults(2–5). Recently, there has been renewed interest in Ross procedure at specialized centers which demonstrated restoration to normal age-matched population survival(6–9). However, autograft dilatation leading to aneurysm formation or valve insufficiency remains challenging(2–5, 10–12). Reintervention for autograft repair or replacement can add significant morbidity to patients(13).

Previously, our group created one realistic human computational model incorporating pulmonary autograft geometry and material properties using finite element (FE) analysis (14). We investigated mechanisms of autograft dilatation by examining wall stresses after exposure to systemic pressure. Wall stress cannot be directly measured but can be determined by computational modeling. Accurate computational models require precise autograft geometry at zero-pressure, patient-specific material properties, and physiologic loading conditions. Our autograft model was based on geometry from micro-computed tomography of a human autograft at zero pressure. Using one human autograft material property, we quantified changes in autograft diameter and wall stress upon exposure to systemic pressure. Autograft diameter increased up to 17% and peak von Mises wall stresses increased nearly 6-fold (48.6 to 289.6kPa). However, the range of autograft biomechanical responses based upon variation in patient-specific autograft material properties is unknown. Furthermore, patient-specific material properties are challenging to determine *in vivo*, requiring costly and time-consuming magnetic resonance imaging with cine displacement encoded imaging with stimulated echoes (DENSE-MRI)(15). Alternatively, patient-specific material properties require surgical excision and tissue for direct measurement *in vitro*(16). We previously demonstrated that pulmonary sinus and artery material properties varied significantly among patients(17). However, our group recently performed FE modeling on ascending aortic aneurysms and found that aneurysm wall stresses were not significantly affected by variation in patient-specific material properties based on *in vivo* FE models(18). However, it is unknown how wall stresses are affected by variation in patient-specific material properties with *ex vivo* FE models. The purpose of this study was to investigate the range of autograft biomechanical responses to systemic pressure by using patient-specific material properties, obtained from biaxial stretch testing of normal human autografts. These results lay the foundation for understanding normal autograft responses upon immediate exposure to systemic pressures. Understanding how variations in patient-specific material properties impact *ex vivo* FE modeling and wall stresses is necessary for future studies examining patient-specific autograft remodeling.

Materials and Methods

Pulmonary Root Tissue Acquisition

A human pulmonary root was obtained from a normal donor heart not used for transplantation via Transplant Donor West (Oakland, CA). Consent was obtained for use for research purposes and patient death was from non-cardiac causes. Acquisition of deidentified human tissue was exempted by Committee on Human Research at University of California San Francisco Medical Center, and its use approved by Institutional Review Board at San Francisco Veterans Affairs Medical Center, and Transplant Donor West.

Pulmonary Root Mesh Generation

Developing a realistic FE model requires accurate three-dimensional autograft geometry, material properties, and physiologic loading conditions. The previously developed pulmonary autograft model was generated as described(14). Briefly, a single human pulmonary root was harvested from valve annulus to just distal to sinotubular junction (STJ). Autograft was fixed upright with 10% dilute formalin for 24 hours to maintain zero-stress geometry and imaged with a cone-beam micro-computed tomography scanner (microCT-40; Scanco Medical AG, Baseldorf, Switzerland).

High resolution DICOM (Digital Imaging and Communications in Medicine) radiologic images of human autograft (voxel size 76×76×76μm) were imported into ITK-SNAP (www.itksnap.org), an open-source automatic image segmentation software(19). Images were filtered using an intensity threshold to isolate autograft geometry. Surface mesh of autograft wall and inner lumen was formed with Rapidform XOR (INUS Technology, Inc., Sunnyvale, CA, USA) excluding valve leaflets. Autograft geometry was discretized into a mesh comprising ~6000 hexahedral elements with mean element volume $0.59\pm0.21 mm^3$(TrueGrid; XYZ Scientific, Inc., Livermore, CA, USA) to create autograft geometry of accurate size and thickness at zero-stress conditions.

Finite Element Analysis

Material properties from normal freshly harvested human pulmonary autograft specimens (n=24) from donors without aortic valve pathology underwent bi-axial stretch testing as previously described(17) to obtain stress-strain data for use in FE model(Figure 1). Mean age of patients from which specimens originated was 50 years old. Ogden hyper-elastic material, previously used to describe non-linear stress-strain relationships in arterial tissues, was chosen to model autograft material properties(14, 20). Ogden non-linear constitutive equation is described as:

$$W(\lambda_1, \lambda_2, \lambda_3) = \sum_{p=1}^{N} \mu_p\left(\lambda_1^{ap} + \lambda_1^{ap} + \lambda_1^{ap} - 3\right)\alpha_p$$

where N, μ_p and α_p are material constant, λ_j are the principal stretches.

LS-DYNA (LSTC, Inc., Livermore, CA, USA), a commercially available explicit FE solver was utilized for autograft simulations and data analysis. We previously demonstrated that human pulmonary roots had no anisotropy, i.e. no differences in stress-strain responses

in circumferential vs. longitudinal directions within the physiologic range, thus autograft material was modeled as isotropic(17). Raw stress-strain data (Figure 1) from pulmonary autograft bi-axial stretch testing was input into LS-DYNA for regression to the Ogden material model.

Pressure loading curves were applied uniformly to autograft inner lumen and were representative of human systemic and pulmonary pressures. Simulations with each set of autograft material properties were run at systemic pressures ranging from 80–120mmHg and pulmonary pressures ranging 8–25mmHg. Two cardiac cycles of 800ms were applied, consisting of 300ms ramp up to maximum systolic pressure, and 500ms decrease to minimum diastolic pressure. Systole comprised 38% of the cardiac cycle. Boundary conditions were used to constrain autograft motion at left ventricular outflow tract/annulus border, while physiological longitudinal stretch was applied to distal end of autograft(21–23). All remaining elements of the autograft were unconstrained.

Post-Processing and Data Analysis

Simulation results were examined at peak systolic and minimum diastolic pressures, where wall stresses and autograft diameters were measured. First (FPS) and second principal (SPS) wall stresses were calculated by LS-DYNA post-processing software. Maximal wall stress and diameters were determined as previously described(14). For element volume analysis, individual element volumes for each autograft model were made available by LS-DYNA. The sum of all element volumes for a given model with FPS or SPS values exceeding a determined threshold was obtained. This value was then divided by the total autograft element volume for each autograft model. All reported values are displayed as mean±standard deviation (SD), and T-test was used to determine significance.

Results

Upon initial pressurization from 0mmHg to pulmonary pressures, autografts underwent large deformation, but pressures >20mmHg did not produce much greater dilation at higher pressures due to increased autograft stiffness. Mean autograft diameters at points in the cardiac cycle for various anatomic regions are listed (Table 1). Autograft distensibility, calculated as ((systolic diameter – diastolic diameter)/diastolic diameter) is reported in Table 2.

Maximal FPS and SPS occurred at systole for both pulmonary and systemic pressure conditions. Regions of maximal wall stress were observed in the sinuses and STJ regions (Figure 2a–b). Influence of individual material properties on wall stress can be appreciated qualitatively in color plots across each of three representative models. Peak and mean FPS and SPS for each pressure condition are shown (Figures 3a–b, 4a–b). Autograft peak and mean FPS/SPS were significantly different under systemic versus pulmonary pressure loading conditions ($p<0.001$).

For element volume analysis, group mean FPS at systemic systole is defined as the mean element FPS value across all 24 autograft models at systemic systole and was 194.81±82.89kPa. Group mean SPS at systemic systole was 131.00±55.62kPa. The

percentage of autograft element volume exceeding group mean FPS was 37.46±6.09%, and autograft element volume exceeding one SD of group mean FPS (threshold: 277.70kPa) was 14.25±5.61%. For SPS, group mean at systemic systole was 131.00±55.62kPa. Mean autograft element volume exceeding SPS group mean was 39.49±13.72% and autograft element volume exceeding one STD of group mean SPS was 12.60±10.13%(Figure 5).

Discussion

Our group has previously developed the first human finite element model of a pulmonary autograft that used precise three-dimensional geometry and human autograft mechanical properties to investigate wall stresses upon immediate exposure to systemic circulation pressures(14). Significant increases in wall stress were quantified but the non-linear characteristic of the material property prevented significant dilation of the autograft. Here we applied 24 different human autograft material properties to our single FE model enabling us to examine based upon a normal range of autograft biomechanical properties, the range of wall stress responses to systemic pressures.

Autograft Dimensions

Autograft had larger dimensions in all regions at systemic than pulmonary pressures. These differences in systolic dimensions between systemic and pulmonary pressures were greatest at the sinuses and STJ (3.49 ±1.63mm, 3.50 ± 1.60mm, respectively) compared to the annulus (1.60 ± 0.69mm). Notably, predicted autograft diameters at systemic pressure demonstrated little variation as evidenced by the narrow standard deviation, suggesting variable material properties led to similar results.

Distensibility was greater at pulmonary pressures (3–9%) than systemic pressures (1–2%), with greatest distensibility occurring at the STJ. Minimal distensibility is explained by the non-linearity of the material properties, where at higher pressures, material stiffness increases to resist further dilatation.

Autograft Wall Stresses

Significantly elevated FPS and SPS were quantified upon exposure to systemic pressure.. The ~five-fold increase in peak FPS existed across all autograft regions, with greatest magnitudes occurring at sinuses and STJ, which correlates with echocardiographic findings(24, 25).

Tissue Biomechanics Studies

We previously studied biomechanics of autografts (mean systolic diameter 45.8±4.0mm) explanted an average of 13.0±2.1years after Ross procedure from patients at Erasmus Medical Center(26, 27). Explanted autografts were less stiff than both normal aortic root at systemic pressure and normal pulmonary roots at pulmonary pressure. Explanted autograft walls were thicker(1.7±0.2mm) than that of normal pulmonary roots(1.0±0.2mm). This finding has also been corroborated by Nappi et al, who elaborated on biomechanical tissue responses accounting for this observation(28, 29). Increased wall thickness may serve as a compensatory mechanism to lessen increased wall stress. Though anover-

simplification, Laplace's law states wall stress is directly proportional to diameter and inversely proportional to thickness.. Our computational results are valuable to suggest that compensatory mechanisms to normalize autograft wall stress after exposure to systemic pressure may include increased wall thickness, based upon our prior studies. Future studies investigating changes in *in vivo* wall thickness after the Ross procedure will be necessary to understand how wall thickness impacts stress results, given the non-linearity of material properties and non-ideal geometry which is assumed with Laplace's law.

Element Volume Stress Analysis

Mean element volume was $0.59\pm0.21 mm^3$ at systemic systole. We utilized a volumetric analysis to better quantify the physical distribution of wall stress within the model itself as well as among the population of models. Use of color plots (Figure 2) provides a visual aid to understand stress distribution within a model, but is limited for comparing a group of models.

The threshold for element volume calculations was chosen as one SD over the group mean FPS and SPS at systemic systole. This mean and SD based on the range of material properties across 24 patients served as a "population threshold" for our study. If patient-specific material properties are not known which is often the case with *in vivo* imaging, autografts with greater percentages of volume exceeding the threshold represented patient-specific outliers whose actual stresses were greater than the predicted stresses. This analysis provides important information on the ability of FE models without patient-specific material properties to accurately predict wall stress values for a given patient. With only 13–14% of autograft element volume experiencing stress outside group mean + oneSD of wall stresses, use of population-averaged material properties could reasonably account for a majority of the autografts elements' response to pressure loading. Using population-averaged material properties coupled with group mean + SD stress values and long-term clinical follow-up, future thresholds may be established correlating autograft aneurysm development with biomechanical wall stresses.

Advances in Surgical Techniques

Over the past decade, advances in surgical techniques and post-operative care have enabled specialized centers to achieve excellent long-term survival with the Ross procedure(2, 3, 5, 10–12, 30). Attention has turned towards identification of patient clinical and anatomic factors that may be associated with autograft dilatation. Aortic annulus dilation has been identified as a significant predictor of autograft dilation(5, 10). Karaskov et al. performed annulus reduction if >27mm or there was >2mm diameter difference between aortic and autograft annulus(5). Brown et al. identified aortic annulus z-value >+2.0 as a significant predictor of autograft dilation, and those patients underwent annulus reduction and fixation with PTFE strip(10). They also replaced dilated ascending aorta with a Dacron graft to support the STJ, to stabilize the STJ.

Autograft external reinforcement has also been practiced. Bansal et al. reported improved 5-year freedom from autograft reintervention from 81% to 91% ($p<0.001$) after routine use of Hemashield autograft support in patients >10 years old(2). Carrel et al. reported 21 of 22

Ross adult patients receivingexternal Dacron graft reinforcement with no autograft dilatation approaching 10-year follow-up(30). Skillington developed autologous support, where in addition to aortic annulus adjustment to match autograft annulus, external reinforcement with the patient's native aorta was used(33). Composite freedom from all reoperations on the aortic valve and greater than mild autograft regurgitation was 93% at 15 years.

Our models suggest that with increased stresses in the sinuses and STJ, external support in these regions may be beneficial to reduce autograft stresses and subsequent dilatation. Nappi et al. have computationally studied limiting autograft length and external reinforcement, with results supportive of shorter autograft lengths withstanding higher pressurization(34). Additionally, they investigated animal models of a bioresorbable scaffold composed of crosslinked polydioaxanone mesh and subsequent histologic autograft remodeling(31, 32). Future computational studies involving FEA and various autograft implant and reinforcement techniques coupled with animal and clinical studies may offer quantitative analyses of how autograft wall stresses are impacted in relationship to aneurysm dilatation.

Primary Valve Pathology, Tissue Properties, and Autograft Dilatation

Controversy exists regarding the influence of bicuspid aortic valve (BAV) vs. tricuspid aortic valve in subsequent autograft dilatation. Biomechanically, on one hand, Mookhoek et al. noted greater autograft wall stiffness at pulmonary pressures in BAV than TAV patients(26, 27). While on the other hand, Dionne et al. found no differences in pulmonary artery mechanical properties of BAV vs. TAV patients undergoing the Ross procedure(16). They did find that pulmonary artery stiffness was greater in aortic stenosis (AS), mixed disease or endocarditis compared to pure aortic regurgitation (AR). Clinically, Brown et al. found no significant difference in autograft dilatation in BAV versus TAV patients, though primary valve pathology was not discussed(10). AR patients appear to be predisposed to autograft dilatation Da Costa et al. found AR as indication for surgery was predictive of autograft root diameter ≥45mm at late follow-up with 86% freedom from root dilatation with AS vs 56% with AR(11). Our study uses material properties from normal autograft specimens without aortic valve pathology. Future studies to investigate the impact of BAV vs TAV, or AS vs AR will be necessary to determine if such aortic valve pathology influences pulmonary autograft material properties or autograft wall stresses. How aortic valve pathology influences autograft mechanical behavior and wall stress distribution may influence clinical decision-making on selecting ideal patients for the Ross procedure or addition of external support.*Study Limitations*

This human pulmonary autograft model described the influence of material properties on wall stresses in *ex vivo* FE modeling incorporating realistic geometry of one autograft and application of blood pressures applied to the inner lumen. Future studies will incorporate both patient-specific geometries with their patient-specific material properties to fully elucidate the influence of geometry vs material properties in wall stress analyses. In addition, this study cannot provide wall stress thresholds to determine if patients should or should not receive Ross operation due to concerns for future aneurysm development. Future *in vivo* FE modeling over time coupled with clinical follow-up for aneurysm formation will be required to answer the predictive value of wall stresses and autograft aneurysm formation.

Valve leaflets were not included, as they did not contribute significantly to the physiologic interactions influencing autograft wall stress. Valve leaflets would be necessary to include if a computational fluid dynamics study was being performed to examine velocity field distribution and flow characteristics, or if investigating fluid-structure interactions and shear stress, which were beyond the scope of this study.

Conclusion

A nearly five-fold increase in peak wall stress was observed at systemic pressures after the Ross operation with regions of peak stresses observed in autograft sinuses and STJ regions, corresponding to clinical regions of autograft dilatation. Volumetric analysis of each autograft based on summation of elements exceeding FPS and SPS threshold based on the group mean was performed. These data improve upon mean and peak stress analysis and provide important data regarding use of population-based material properties to predict patient-specific mechanical behavior. Future investigation of patient-specific human autografts using patient-specific geometry and material properties will further elucidate not only the degree of wall stress change from pulmonary to systemic pressure.

Acknowledgements

This study was funded by NIH R01HL119857–01A1, administered by the Northern California Institute for Research and Education using resources of the San Francisco Veterans Affairs Medical Center. We appreciate heart specimen collection from Transplant Donor West.

References

1. Ross DN. Replacement of aortic and mitral valves with a pulmonary autograft. Lancet (London, England) 1967;2(7523):956–8.
2. Bansal N, Kumar SR, Baker CJ, Lemus R, Wells WJ, Starnes VA. Age-Related Outcomes of the Ross Procedure Over 20 Years. The Annals of thoracic surgery 2015;99(6):2077–83; discussion 84–5. [PubMed: 25921257]
3. Kalfa D, Mohammadi S, Kalavrouziotis D, et al. Long-term outcomes of the Ross procedure in adults with severe aortic stenosis: single-centre experience with 20 years of follow-up. European journal of cardio-thoracic surgery : official journal of the European Association for Cardio-thoracic Surgery 2015;47(1):159–67; discussion 67. [PubMed: 24574445]
4. Takkenberg JJ, Klieverik LM, Schoof PH, et al. The Ross procedure: a systematic review and meta-analysis. Circulation 2009;119(2):222–8. [PubMed: 19118260]
5. Karaskov A, Sharifulin R, Zheleznev S, Demin I, Lenko E, Bogachev-Prokophiev A. Results of the Ross procedure in adults: a single-centre experience of 741 operations. European journal of cardio-thoracic surgery : official journal of the European Association for Cardio-thoracic Surgery 2016;49(5):e97–e104. [PubMed: 27130952]
6. El-Hamamsy I, Eryigit Z, Stevens LM, et al. Long-term outcomes after autograft versus homograft aortic root replacement in adults with aortic valve disease: a randomised controlled trial. Lancet (London, England) 2010;376(9740):524–31.
7. Mokhles MM, Rizopoulos D, Andrinopoulou ER, et al. Autograft and pulmonary allograft performance in the second post-operative decade after the Ross procedure: insights from the Rotterdam Prospective Cohort Study. European heart journal 2012;33(17):2213–24. [PubMed: 22730489]
8. El-Hamamsy I, Bouhout I. The Ross procedure: time for a hard look at current practices and a reexamination of the guidelines. Annals of translational medicine 2017;5(6):142. [PubMed: 28462222]

9. Um KJ, McClure GR, Belley-Cote EP, et al. Hemodynamic outcomes of the Ross procedure versus other aortic valve replacement: a systematic review and meta-analysis. The Journal of cardiovascular surgery 2018;59(3):462–70. [PubMed: 29327563]
10. Brown JW, Ruzmetov M, Rodefeld MD, Mahomed Y, Turrentine MW. Incidence of and risk factors for pulmonary autograft dilation after Ross aortic valve replacement. The Annals of thoracic surgery 2007;83(5):1781–7; discussion 7–9. [PubMed: 17462399]
11. Costa FD, Colatusso DF, Balbi Filho EM, et al. 20 years experience with the Ross operation in middle-aged patients: the autologous principle is still alivedagger. Interactive cardiovascular and thoracic surgery 2017;24(3):348–54. [PubMed: 28017933]
12. Skillington PD, Mokhles MM, Takkenberg JJ, et al. Twenty-year analysis of autologous support of the pulmonary autograft in the Ross procedure. The Annals of thoracic surgery 2013;96(3):823–9. [PubMed: 23870828]
13. David TE. Ross procedure at the crossroads. Circulation 2009;119(2):207–9. [PubMed: 19153280]
14. Wisneski AD, Matthews PB, Azadani AN, et al. Human pulmonary autograft wall stress at systemic pressures prior to remodeling after the Ross procedure. The Journal of heart valve disease 2014;23(3):377–84. [PubMed: 25296465]
15. Krishnan K, Ge L, Haraldsson H, et al. Ascending thoracic aortic aneurysm wall stress analysis using patient-specific finite element modeling of in vivo magnetic resonance imaging. Interact Cardiovasc Thorac Surg 2015;21(4):471–80. [PubMed: 26180089]
16. Dionne PO, Wener E, Emmott A, et al. The Ross procedure: biomechanical properties of the pulmonary artery according to aortic valve phenotype. Interactive cardiovascular and thoracic surgery 2016;23(3):371–6. [PubMed: 27241051]
17. Azadani AN, Chitsaz S, Matthews PB, et al. Regional mechanical properties of human pulmonary root used for the Ross operation. The Journal of heart valve disease 2012;21(4):527–34. [PubMed: 22953683]
18. Wang Z, Xuan Y, Guccione JM, Tseng EE, Ge L. Impact of patient-specific material properties on aneurysm wall stress: Finite element study. The Journal of heart valve disease 2018;(In Press).
19. Yushkevich PA, Piven J, Hazlett HC, et al. User-guided 3D active contour segmentation of anatomical structures: significantly improved efficiency and reliability. NeuroImage 2006;31(3):1116–28. [PubMed: 16545965]
20. Lally C, Reid AJ, Prendergast PJ. Elastic behavior of porcine coronary artery tissue under uniaxial and equibiaxial tension. Annals of biomedical engineering 2004;32(10):1355–64. [PubMed: 15535054]
21. Matthews PB, Jhun CS, Yaung S, et al. Finite element modeling of the pulmonary autograft at systemic pressure before remodeling. The Journal of heart valve disease 2011;20(1):45–52. [PubMed: 21404897]
22. Han HC, Fung YC. Longitudinal strain of canine and porcine aortas. Journal of biomechanics 1995;28(5):637–41. [PubMed: 7775500]
23. Grande-Allen KJ, Cochran RP, Reinhall PG, Kunzelman KS. Re-creation of sinuses is important for sparing the aortic valve: a finite element study. The Journal of thoracic and cardiovascular surgery 2000;119(4 Pt 1):753–63. [PubMed: 10733765]
24. Carr-White GS, Afoke A, Birks EJ, et al. Aortic root characteristics of human pulmonary autografts. Circulation 2000;102(19 Suppl 3):Iii15–21. [PubMed: 11082356]
25. Hokken RB, Bogers AJ, Taams MA, et al. Does the pulmonary autograft in the aortic position in adults increase in diameter? An echocardiographic study. The Journal of thoracic and cardiovascular surgery 1997;113(4):667–74. [PubMed: 9104975]
26. Mookhoek A, Krishnan K, Chitsaz S, et al. Biomechanics of Failed Pulmonary Autografts Compared to Native Aortic Roots. The Annals of thoracic surgery 2017;103(5):1482–8. [PubMed: 27765169]
27. Mookhoek A, Krishnan K, Chitsaz S, et al. Biomechanics of Failed Pulmonary Autografts Compared With Normal Pulmonary Roots. The Annals of thoracic surgery 2016;102(6):1996–2002. [PubMed: 27457832]
28. Nappi F, Carotenuto AR, Di Vito D, Spadaccio C, Acar C, Fraldi M. Stress-shielding, growth and remodeling of pulmonary artery reinforced with copolymer scaffold and transposed into

aortic position. Biomechanics and modeling in mechanobiology 2016;15(5):1141–57. [PubMed: 26603438]

29. Nappi F, Carotenuto AR, Cutolo A, et al. Compliance mismatch and compressive wall stresses drive anomalous remodelling of pulmonary trunks reinforced with Dacron grafts. Journal of the mechanical behavior of biomedical materials 2016;63:287–302. [PubMed: 27442920]
30. Carrel T, Kadner A. Long-Term Clinical and Imaging Follow-Up After Reinforced Pulmonary Autograft Ross Procedure. Seminars in thoracic and cardiovascular surgery Pediatric cardiac surgery annual 2016;19(1):59–62. [PubMed: 27060045]
31. Nappi F, Spadaccio C, Fraldi M, et al. A composite semiresorbable armoured scaffold stabilizes pulmonary autograft after the Ross operation: Mr Ross's dream fulfilled. The Journal of thoracic and cardiovascular surgery 2016;151(1):155–64.e1. [PubMed: 26602900]
32. Spadaccio C, Montagnani S, Acar C, Nappi F. Introducing bioresorbable scaffolds into the show. A potential adjunct to resuscitate Ross procedure. International journal of cardiology 2015;190:50–2. [PubMed: 25912121]
33. Skillington PD, Mokhles MM, Takkenberg JJ, et al. The Ross procedure using autologous support of the pulmonary autograft: techniques and late results. The Journal of thoracic and cardiovascular surgery 2015;149(2 Suppl):S46–52. [PubMed: 25439787]
34. Nappi F, Nenna A, Larobina D, et al. Simulating the ideal geometrical and biomechanical parameters of the pulmonary autograft to prevent failure in the Ross operation. Interactive cardiovascular and thoracic surgery 2018;27(2):269–76. [PubMed: 29538653]

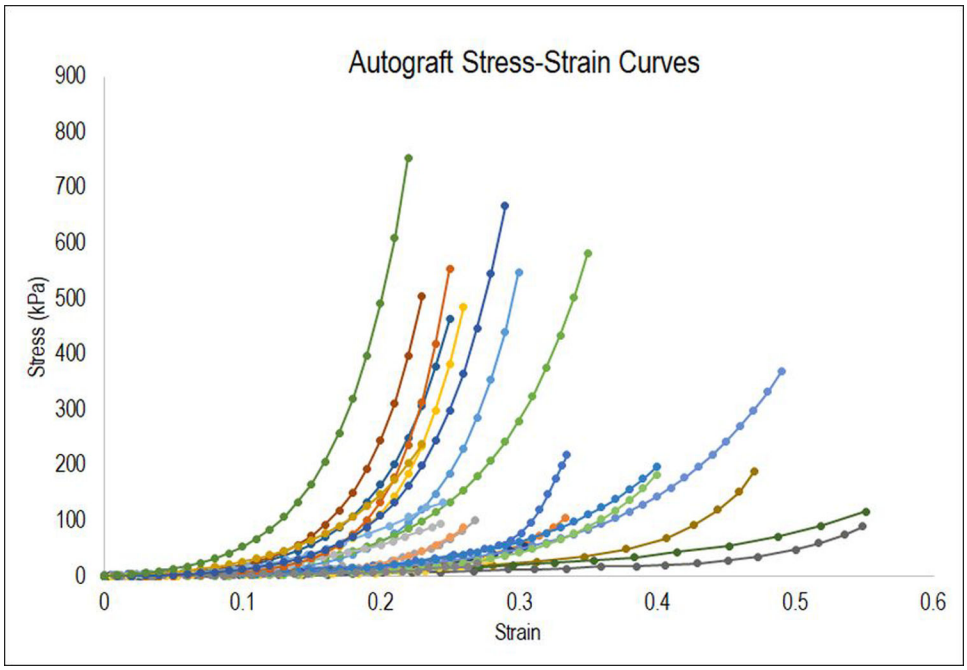

Figure 1.
Equiaxial stretch data from pulmonary autografts.

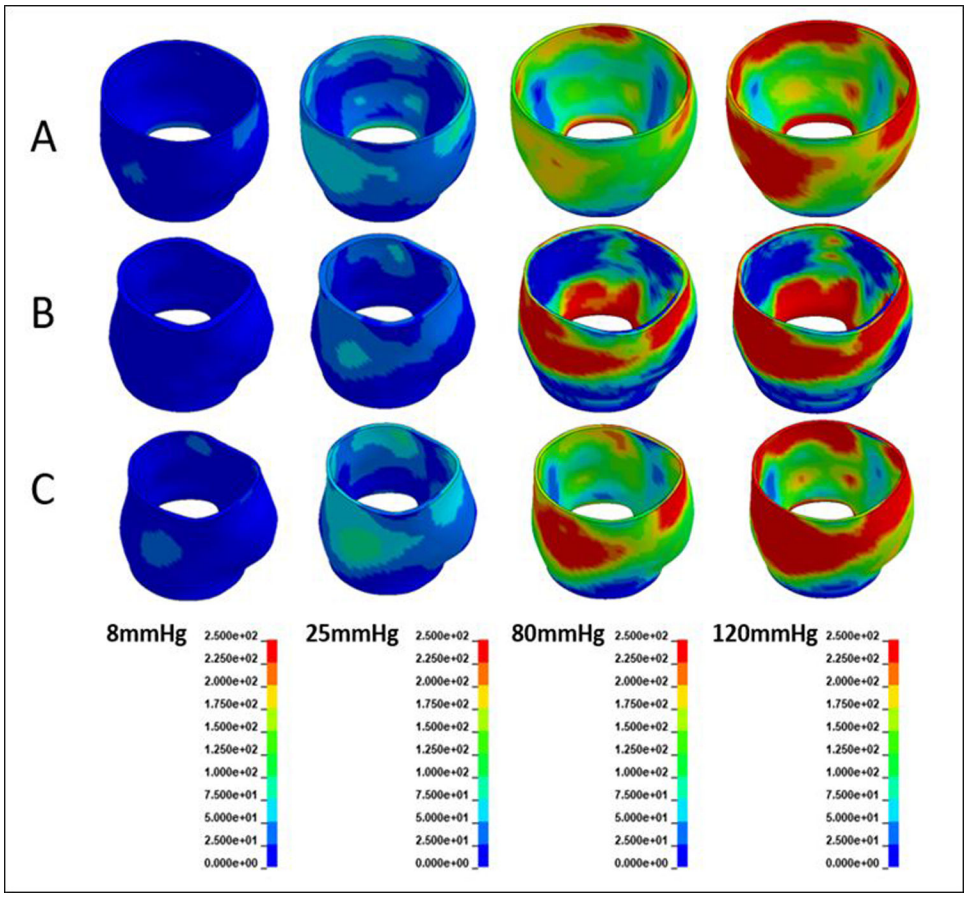

Figure 2a.

Pulmonary autograft first principal wall stresses at pulmonary and systemic pressures. Three representative autografts are shown (A, B, C) at various pressures. Color bar indicates ranges of wall stress (kPa) in the autograft.

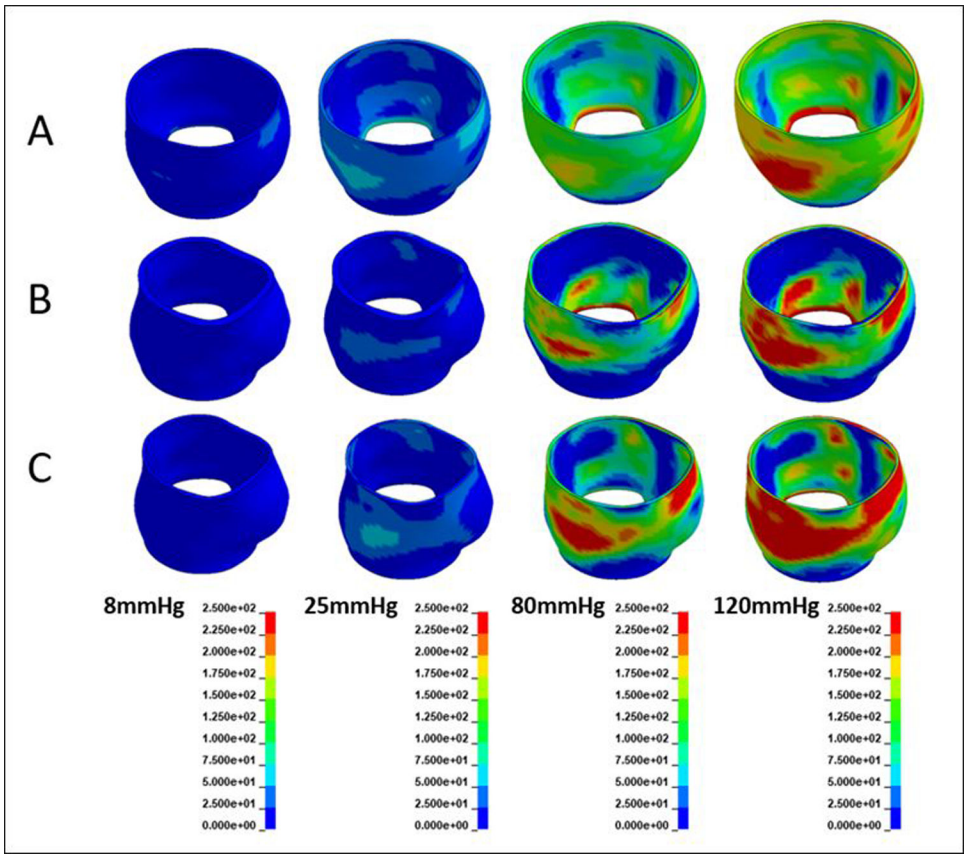

Figure 2b.

Pulmonary autograft second principal wall stresses at pulmonary and systemic pressures. Representative autografts (n=3) are shown (A, B, C). Color bar indicates ranges of autograft wall stress(kPa).

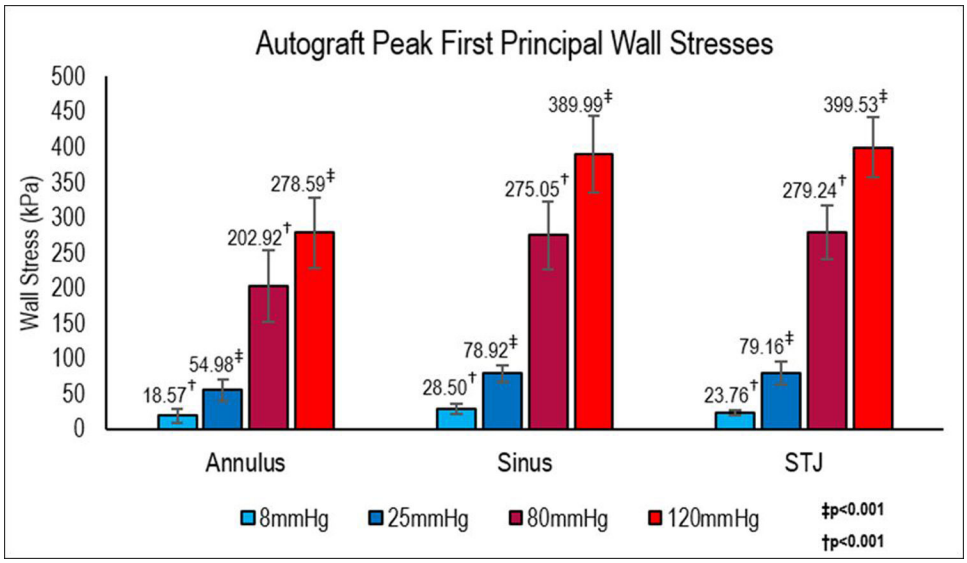

Figure 3a.

Peak FPS values at autograft regions at pulmonary and systemic pressures. All differences in peak FPS for a given autograft region are statistically significant ($p<0.001$) when pressure environment changed.

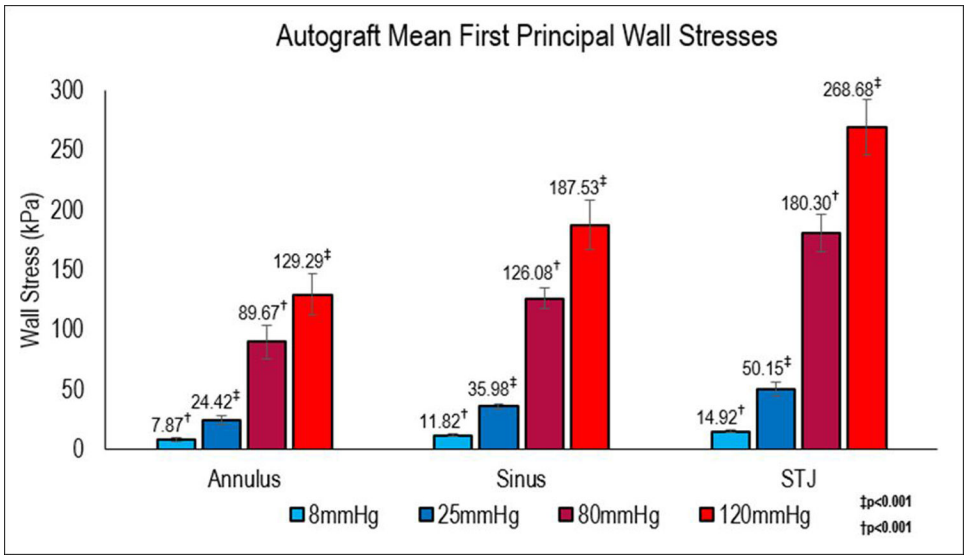

Figure 3b.

Peak SPS values at autograft regions at pulmonary and systemic pressures. All differences in peak SPS for a given autograft region are statistically significant ($p<0.001$) when pressure environment changed.

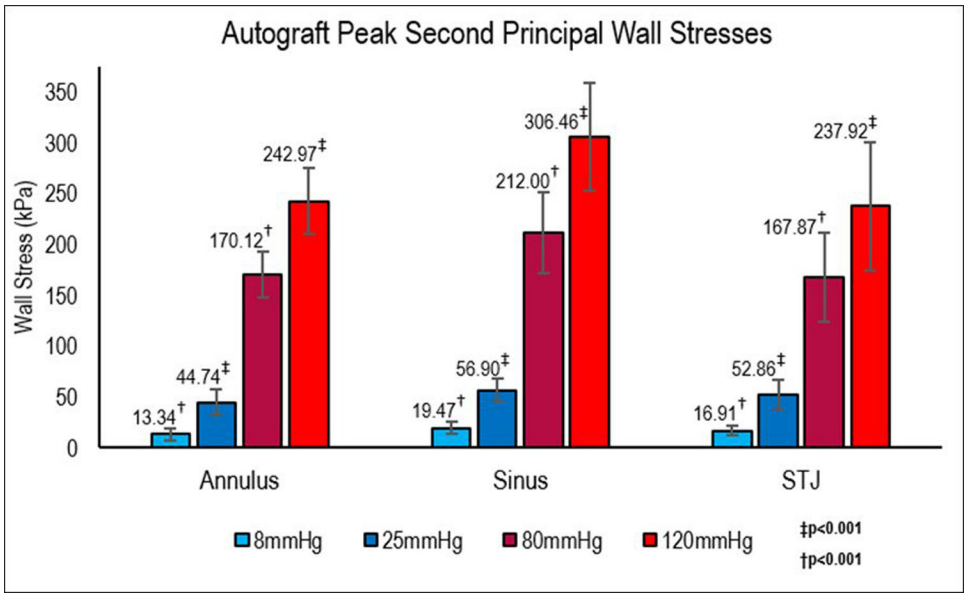

Figure 4a.

Mean FPS values at autograft regions at pulmonary and systemic pressures. All differences in peak FPS for a given autograft region and pressure phase are statistically significant ($p<0.001$) when pressure environment changed.

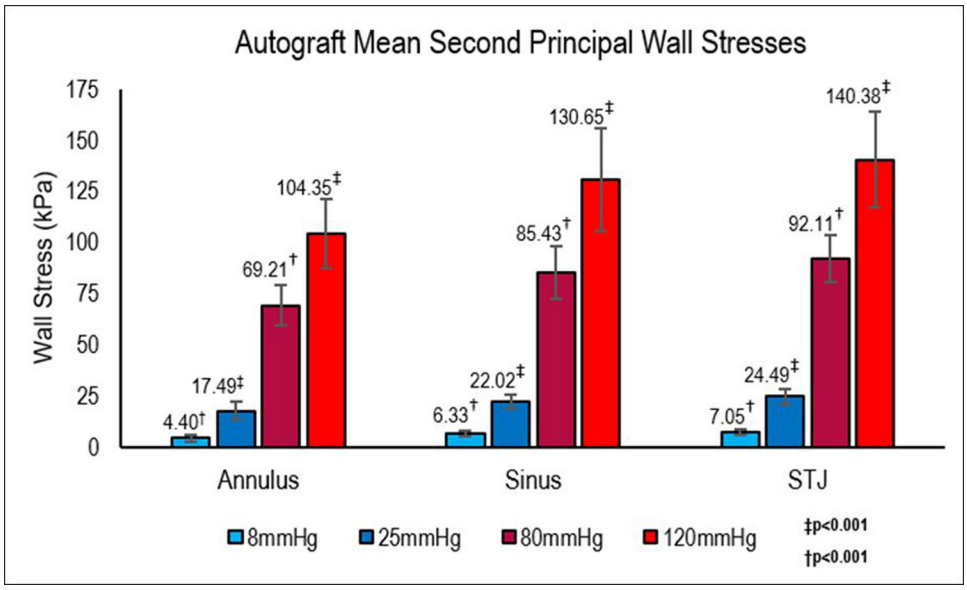

Figure 4b.

Mean SPS values at autograft regions at pulmonary and systemic pressures. All differences in peak SPS for a given autograft region and pressure phase are statistically significant ($p<0.001$) when pressure environment changed.

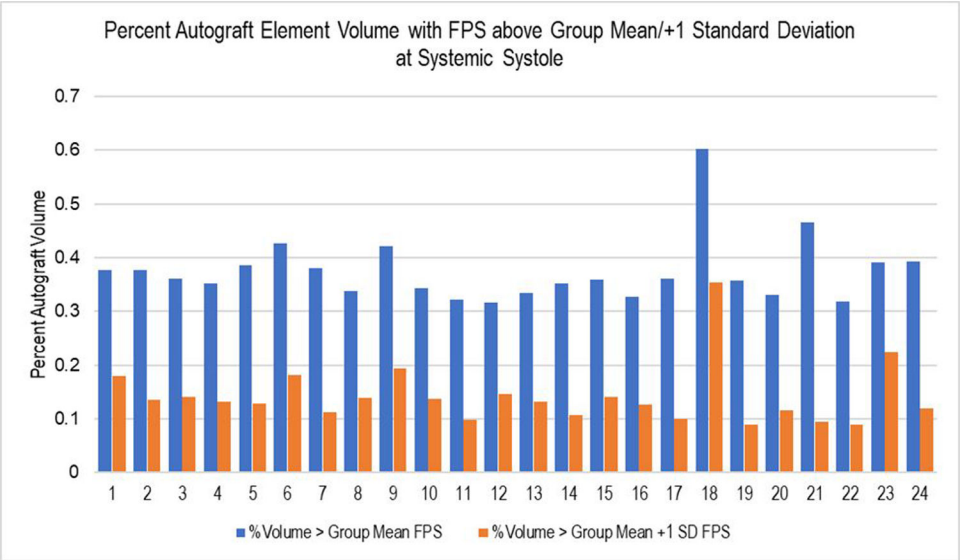

Figure 5a.

Percent volume of autograft elements with FPS values exceeding the group mean FPS values, and exceeding group mean + 1 standard deviation FPS values.

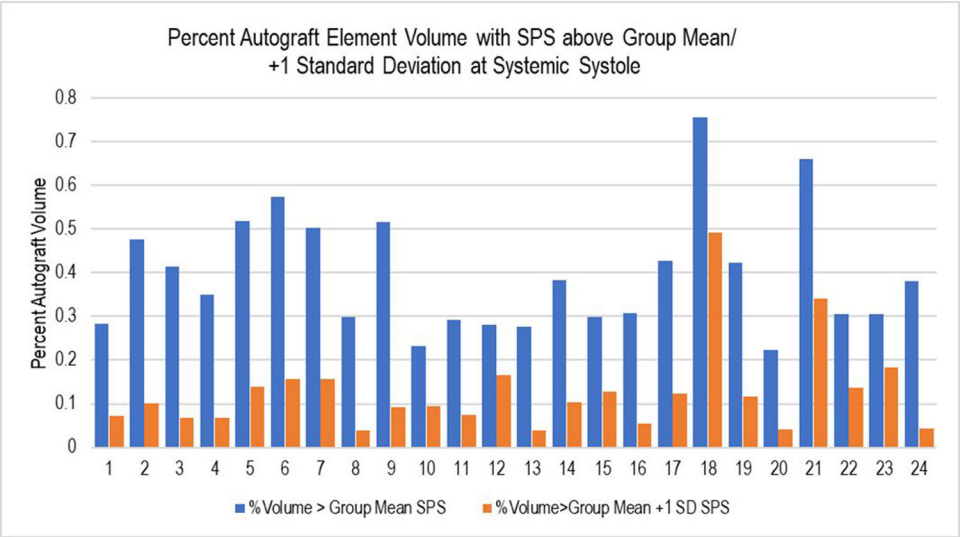

Figure 5b.

Percent volume of autograft elements with SPS values exceeding the group mean SPS values, and exceeding group mean + 1 standard deviation SPS values.

Table 1.

Diameters (mm) of autograft regions at pulmonary and systemic pressures.

	Pulmonary pressures		Systemic pressures	
Regions	**8mmHg**	**25mmHg**	**80mmHg**	**120mmHg**
Annulus	33.47±0.67	34.35±1.01	35.58±1.18	35.95±1.34
Sinus	32.71±2.04	35.14±2.93	37.84±2.85	38.64±3.21
STJ	31.66±1.77	34.40±2.47	37.11±2.47	37.90±2.83

STJ: sinotubular junction

Table 2.

Distensibility of autograft regions at pulmonary and systemic pressures expressed as a percentage.

Regions	Pulmonary pressures	Systemic pressures
Annulus	2.64±1.74%†	1.02±0.55%†
Sinus	7.48±6.77%‡	2.07±1.16%‡
STJ	8.75±7.51%*	2.11±1.10%*

STJ: sinotubular junction.

† p<0.001.

‡ p<0.001.

* p<0.001.